the FEBS Journal

Crystal structure of a ring-cleaving cyclohexane-1,2-dione hydrolase, a novel member of the thiamine diphosphate enzyme family

Alma Steinbach[1], Sonja Fraas[1], Jens Harder[2], Eberhard Warkentin[3], Peter M. H. Kroneck[1] and Ulrich Ermler[3]

1 Fachbereich Biologie, Mathematisch-Naturwissenschaftliche Sektion, Universität Konstanz, Germany
2 Max-Planck-Institut für Marine Mikrobiologie, Bremen, Germany
3 Max-Planck-Institut für Biophysik, Frankfurt, Germany

Keywords
alicyclic compounds; anaerobic degradation; cyclohexane-1,2-dione hydrolase; enzyme catalysis; ThDP

Correspondence
P. M. H. Kroneck, Fachbereich Biologie, Mathematisch-Naturwissenschaftliche Sektion, Universität Konstanz, 78457 Konstanz, Germany
Fax: +49 7531 88 2966
Tel: +49 7531 88 4112
E-mail: peter.kroneck@uni-konstanz.de
U. Ermler, Max-Planck-Institut für Biophysik, Max-von-Laue-Str. 3, 60438 Frankfurt, Germany
Fax: +49 69 6303 1002
Tel: +49 69 6303 1054
E-mail: ulermler@biophys.mpg.de

(Received 2 December 2011, revised 23 January 2012, accepted 1 February 2012)

doi:10.1111/j.1742-4658.2012.08513.x

The thiamine diphosphate (ThDP) dependent flavoenzyme cyclohexane-1,2-dione hydrolase (CDH) (EC 3.7.1.11) catalyses a key step of a novel anaerobic degradation pathway for alicyclic alcohols by converting cyclohexane-1,2-dione (CDO) to 6-oxohexanoate and further to adipate using NAD^+ as electron acceptor. To gain insights into the molecular basis of these reactions CDH from denitrifying anaerobe *Azoarcus* sp. strain 22Lin was structurally characterized at 1.26 Å resolution. Notably, the active site funnel is rearranged in an unprecedented manner providing the structural basis for the specific binding and cleavage of an alicyclic compound. Crucial features include a decreased and displaced funnel entrance, a semi-circularly shaped loop segment preceding the C-terminal arm and the attachment of the C-terminal arm to other subunits of the CDH tetramer. Its structural scaffold and the ThDP activation is related to that observed for other members of the ThDP enzyme family. The selective binding of the competitive inhibitor 2-methyl-2,4-pentane-diol (MPD) to the open funnel of CDH reveals an asymmetry of the two active sites found also in the dimer of several other ThDP dependent enzymes. The substrate binding site is characterized by polar and non-polar moieties reflected in the structures of MPD and CDO and by three prominent histidine residues (His28, His31 and His76) that most probably play a crucial role in substrate activation. The NAD^+ dependent oxidation of 6-oxohexanoate remains enigmatic as the redox-active cofactor FAD seems not to participate in catalysis, and no obvious NAD^+ binding site is found. Based on the structural data both reactions are discussed.

Database
Structural data are available in the Protein Data Bank database under accession number 2PGO

Structured digital abstract
- **CDH** and **CDH** bind by x-ray crystallography (View interaction)

Abbreviations
CDH, cyclohexane-1,2-dione hydrolase; CDO, cyclohexane-1,2-dione; MPD, 2-methyl-2,4-pentane-diol; ThDP, thiamine diphosphate.

Introduction

Thiamine diphosphate (ThDP) dependent enzymes use common structural and mechanistic principles to catalyse a broad range of C–C, C–N, C–S and C–O formation/cleavage reactions [1,2]. Detailed structural information is available for several members of this family, such as transketolase [3], pyruvate oxidase [4] and pyruvate decarboxylase [5], which were its first structurally characterized representatives. All of them are organized as homodimers or homotetramers (dimer of dimers) whereby each monomer is composed of three domains of the α/β type. ThDP, the biologically active derivative of vitamin B1, binds in a V-shaped conformation into a cleft between two subunits which defines the homodimer as essential for catalytic activity [3]. The catalytic power of most ThDP dependent enzymes is based on an inversion of the polarity of the substrate carbonyl group from a partially positive carbon atom into a potentially electron-rich centre capable of donating electrons. This process, called 'Umpolung' is realized by covalent coupling between the deprotonated/activated C2 atom of the thiazolium ring of ThDP and a carbonyl carbon of the substrate. The required ThDP-ylide is formed after abstraction of the C2 proton by the neighbouring 4′-imino group of the pyrimidine ring of ThDP [6]. The energetically unfavoured 4′-imino state is stabilized relative to the 4′-amino state by a proton relay chain between the 4′-N and the 1′-N sites supported by a conserved glutamate residue that abstracts the additional 1′-N proton of the 4′-imino tautomer [7,8]. Solely in glyoxylate carboligase this glutamate is replaced by valine [9]. Many ThDP dependent enzymes exhibit hysteretic activation of ThDP and negative cooperativity in binding their substrates [10] which presuppose a communication between the two spatially separated active sites of the dimer. Several coupling mechanisms have been postulated for enzymes using a ping-pong type mechanism in which the two half reactions proceed alternately in the two active sites like a two-stroke engine [11].

Despite their relative structural and mechanistic uniformity ThDP dependent enzymes participate in many different biosynthetic pathways in all kingdoms of life by various lyase and ligase reactions [12]; some of them open promising perspectives for biotechnological applications [13]. In addition, some members of this enzyme family couple the ThDP dependent reaction with a redox reaction and therefore bind close to the ThDP molecule a redox cofactor that is frequently FAD but in special cases also lipoic acid or an Fe/S cluster [14]. However, in a few ThDP/FAD dependent enzymes, such as acetohydroxy acid synthase and glyoxylate carboligase, FAD appears to solely maintain the structural integrity of the protein, without direct participation in catalysis [15,16].

Our studies are focused on cyclohexane-1,2-dione hydrolase (CDH) isolated from *Azoarcus* strain 22Lin, which is the first ThDP dependent enzyme characterized to date that cleaves an alicyclic ring compound [17,18]. A similar cleavage of a cyclic compound, the conversion of 3D-(3,5/4)-trihydroxycyclohexane-1,2-dione to 5-deoxy-D-glucuronic acid, was described as a reaction step of the myo-inositol catabolism in *Bacillus subtilis* [19]. The enzyme encoded by *iolD* showed the highest relationship to the ThDP dependent enzymes acetolactate synthase from *Spirulina platensis* and *Synechococcus* sp. (26.4% and 26.0% sequence identity) [20]. However, this enzyme has not yet been purified and characterized. In the CDH reaction cyclohexane-1,2-dione (CDO) is hydrolysed to 6-oxohexanoate and the latter is subsequently oxidized to adipate at the expense of NAD^+ (Fig. 1). CDH follows Michaelis–Menten kinetics ($k_{cat,app}$ = 1.6 ± 0.1 s^{-1}, $K_{M,app}$ = 13.3 ± 0.1 μM, and $k_{cat,app}/K_{M,app}$ = 1.2 ± 0.1 × 10^5 $s^{-1}\cdot M^{-1}$ for CDO, and $k_{cat,app}$ = 1.5 ± 0.1 s^{-1}, $K_{M,app}$ = 164 ± 31 μM, $k_{cat,app}/K_{M,app}$ = 0.91 × 10^4 $s^{-1}\cdot M^{-1}$ for NAD^+) and contains one ThDP, one Mg^{2+} and one FAD molecule per monomer [18] in agreement with the primary structure fingerprints for the ThDP and FAD binding sites [21,22]. As reported for the acetohydroxy acid synthase and glyoxylate carboligase [15,16] the FAD cofactor resists reduction under normal physiological conditions but can be partly reduced with the deazaflavin/oxalate system ($E^{\circ\prime}$ = −0.65 V). Sequence comparison studies revealed acetohydroxy acid synthases, glyoxylate carboxylase and cytochrome pyruvate dehydrogenases as closest relatives of CDH, the sequence identities being in the range of approximately 25%. CDH is the key enzyme of a novel anaerobic degradation pathway [17,23] of alicyclic alcohols as the conventional oxidation and hydrolysis pathway is not feasible due to the 1,2 position of two hydroxyl groups [24].

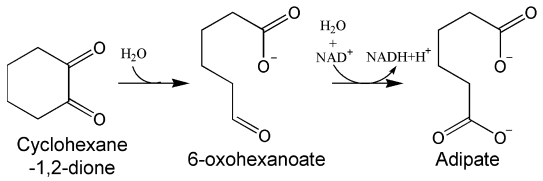

Fig. 1. Reaction of CDH. The ThDP dependent enzyme catalyses the conversion of CDO to adipate; CDH was discovered in the denitrifying anaerobe *Azoarcus* sp. strain 22Lin which metabolizes alicyclic alcohols [17].

Cyclohexane-1,2-diol is a degradation product of steroids, terpenes and other cyclic compounds produced in large amounts by, for example, plants as secondary metabolites. The diol group is oxidized in a first step to the corresponding diketone by two NAD^+ dependent oxidation reactions forming CDO, the substrate of CDH.

In the present work we describe the structure, the cofactor binding and the architecture of the active site funnel of CDH in comparison with other ThDP dependent enzymes. The binding characteristics of the competitive inhibitors 2-methyl-2,4-pentane-diol (MPD) and chloride anion mimicking CDO binding allow the identification of catalytic relevant residues and the postulation of an enzymatic mechanism. The binding of MPD exclusively to one substrate binding funnel of the CDH dimer and the NAD^+ dependent oxidation of 6-oxohexanoate to adipate are discussed.

Results and Discussion

Overall structure

The crystal structure of CDH from *Azoarcus* sp. strain 22Lin has been determined at 1.26 Å resolution by the multiple isomorphous replacement with anomalous scattering (MIRAS) method and refined to R_{cryst} and R_{free} factors of 10.0% and 12.2%, respectively (Table 1). Accordingly, CDH is a homotetrameric enzyme that is composed of a dimer of two dimers arranged in a pseudo 222 symmetric form. The two monomers of the functional dimer forming two complete active sites are referred to as A and B. Each monomer is built up of the domains α (residues 2–182), β (183–372) and γ (373–588); all three are folded as an open α/β structure with six β-strands flanked by α-helices (Fig. 2). This structural organization is characteristic for ThDP-containing enzymes [3,25] which vary, however, in their quaternary structures. Some members are present as dimers and others as tetramers, the latter with variable dimer–dimer orientations. For example, the dimer–dimer orientation deviates by about 15° between CDH and *Lactobacillus plantarum* pyruvate oxidase [4].

Structure comparison studies of the monomers using the Dali server [26] classified CDH as a member of the pyruvate oxidase subfamily documented in low rmsd of 2.3 Å, 2.4 Å, 2.3 Å and 2.3 Å (for 93%, 91%, 89% and 85% of the C_α atoms) to *Arabidopsis thaliana* acetohydroxy acid synthase [27], *Escherichia coli* glyoxylate carboligase [9], *Pseudomonas fluorescens* benzaldehyde lyase [28] and *E. coli* pyruvate dehydrogenase [29], respectively. The sequence identity between CDH and the mentioned most related ThDP enzymes is 23%, 23%, 24% and 22%, respectively. Substantial differences between them exist solely at their 40 C-terminal residues (Fig. 2). In CDH, the segment between residues 550 and 564 is an essential component of the active side funnel (see below) whereas the following stretch (565–581) as well as a short 3_{10}-helix (582–586) link the C-terminal segment with the opposing monomer and the second dimer. The oligomeric contact area is substantially increased by the two C-terminal stretches (565–581) from different dimers that are arranged in a parallel manner over a length of 30 Å (Fig. S1). The interface area buried by the C-terminal arm (565–586) is approximately 1550 $Å^2$ which is more than 25% of the total interdimer contact area.

Substrate funnel

The active site in front of the C2 atom of ThDP is located at the bottom of a 15 Å long, partly narrow funnel (Figs 2, 3) composed of a unique hydrophobic region at its entrance and a more hydrophilic base. The latter is mainly formed by loops following strands B21:B25, B71:B76 and B96:B102 of domain α, by parts of helix A482:A491 of domain γ and by the cofactors ThDP and FAD. The hydrophobic region is composed of the loop connecting strand A253:A256 and helix A263:A271 of helix A482:A490 and, in particular, of a semi-circularly arranged loop close to the C-terminal segment (Fig. 3). This funnel region is coated by apolar side chains of PheA259, LeuA487, LeuA551, ProA561, LeuA563 and LeuA564 that also define the size of the entrance. Interestingly, the funnel architecture in CDH is designed significantly differently than in other ThDP dependent enzymes where the funnel instead corresponds to a cleft characterized by a wide entrance which is mostly displaced by 5–10 Å and lies directly at the monomer–monomer interface (Fig. 3). In CDH, this access is essentially blocked by the semi-circularly shaped loop and the bulky side chain of TrpA285. These new features provide the molecular basis to enlarge the substrate specificity of the ThDP dependent enzyme family to alicyclic diketones. A comparison between CDH, benzaldehyde lyase and benzoylformate decarboxylase indicates no correlation between the geometry of the substrate binding funnel and their similarly large substrates.

Notably, only one substrate funnel is open and provides an oval entrance with a diameter of 7 Å which is sufficiently wide to be passed by CDO (Fig. S1). The other funnel is closed due to small rearrangements (below 2.5 Å) of PheA259, LeuA487, LeuA551 and LeuA563 positioned at the bottleneck of the substrate

Table 1. Data collection and refinement statistics. 'Pip', di-μ-iodobis(ethyldiamine)-di-platinum nitrate; 'terpi', platinum(II) (2,2′:6′,2″-terpyridine) chloride. $R_{sym} = \Sigma | I_i - \langle I \rangle | / \Sigma I_i$, where I_i is the observed intensity and $\langle I \rangle$ is the averaged intensity obtained from multiple observations of symmetry-related reflections. Phasing power (iso) is $\Sigma_n | F_H | / \Sigma_n | E |$ where $| F_H |$ is the calculated structure factor amplitude of the heavy atom structure and E is the lack of closure error; phasing power (ano) is $2\Sigma_n | F_H'' | / \Sigma_n | E |$ where $| F_H'' |$ is the anomalous contribution amplitude. $R_{cryst} = \Sigma_{hkl} (| F_{obs} | - | F_{calc} |) / \Sigma_{hkl} | F_{obs} |$. $R_{free} = R_{cryst}$ with 5% of the observed reflections selected randomly.

	ID14-4 High res.	ID14-4 Low res.	ID14-4 $HgAc_2$ peak	ID14-4 K_2PtCl_4 peak	'Pip'	'Terpy'	ID29 cubic crystals
Crystal properties							
Soaking conditions (mM; h)			0.48; 18.0	0.24; 1.5	0.4; 27	0.2; 4	
Space group	$P4_12_12$						$I432$
Cell constants (Å)	123.6, 144.3						211.0
Solvent content (%)	42.5						59.4
Data collection							
Wavelength (Å)	0.939	0.939	1.005	1.072	1.542	1.542	0.979
Resolution (Å)	1.26	1.7	2.5	2.8	2.7	2.7	3.0
Multiplicity	7.6	6.2	5.8	9.2	5.1	6.5	4.4
Completeness (%)	80.1	93.3	95.7	89.6	98.6	98.2	91.9
R_{sym} (%)	8.6	5.2	4.0	4.9	16.5	7.8	15.9
I/σ_I (last shell)	18.7 (6.1)	24.4 (10.9)	30.9 (18.2)	35.4 (19.6)	9.3 (5.7)	19.9 (12.3)	11.5 (3.0)
Phasing power (iso) (centrics/acentrics)			0.3/0.3	0.3/0.3	0.8/0.9	1.2/1.3	
Phasing power (ano) (centrics/acentrics)			–/1.0	–/1.0	–/–	–/–	
Refinement							
R_{cryst} (%)	10.0						21.0
R_{free} (%)	12.2						25.4
No. of reflections	275 663						66 826
No. of protein atoms	4444						4444
Average *B*-factor (Å^2), protein, ThDP, FAD	9.8, 4.7, 4.9						52
Bond length rms (Å)	0.016						0.008
Bond angle rms (°)	1.66						1.35

funnel. These define a cavity that is inaccessible for bulk solvent and contains sufficient space to accommodate the substrate CDO (Fig. 3). In the structure derived from the cubic crystal form the size of the entrance lies between those observed in the tetragonal form.

Despite the architectural differences of the substrate binding sites the shuttling between open and closed conformations and the crucial function of the C-terminal segment are also reported for other family members. For example, in yeast acetohydroxy acid synthase [30] the partly disordered C-terminal segment in the open state becomes ordered in the closed state to a two-stranded β-sheet followed by a loop-helix structure. Likewise, in oxalyl-CoA decarboxylase [31] a similar rigidification of the C-terminal segment is postulated. In contrast, in CDH both the open and the closed states are conformationally well defined, presumably due to the stabilization of the semi-circularly arranged loop by the C-terminal arm firmly anchored to other monomers of the tetramer (Fig. S1). This fixation concept opens perspectives for a specific reconstruction of the mentioned pronounced loop to realize new substrate specificities for ThDP dependent enzymes in a region between two rigid entities.

Cofactor binding sites

ThDP is strongly anchored to the protein matrix by a divalent metal ion determined as Mg^{2+} in CDH by inductively coupled plasma mass spectrometric measurements [18]. Mg^{2+} ligates to two phosphate oxygens of the pyrophosphate tail, a water molecule, the main chain oxygen of SerA480 and the side chains of AspA451 and AsnA478, the latter being constituents of the conserved ThDP fingerprint motif (Fig. 4) [21]. The thiazolium and methylaminopyrimidine rings are arranged in the characteristic V conformation held in place by a large hydrophobic aliphatic side chain as a leucine in CDH, transketolase [3] and benzoylformate decarboxylase [32] that projects between the two rings and contacts both. The V conformation forces the N4′ atom of pyrimidine in close proximity to the C2 atom of the thiazolium (3.2 Å in CDH) that favours an abstraction of the C2 proton by the N4′ atom and

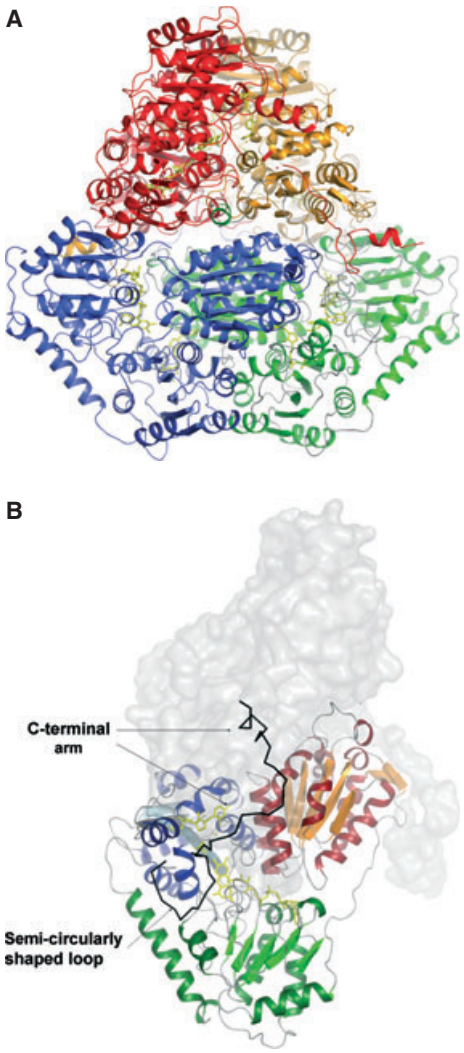

Fig. 2. Structure of the CDH. (A) As tetramer: the subunits are coloured in red/orange and blue/green. (B) As dimer: the three domains of one subunit shown in blue, red and green are essentially composed of a central six-stranded parallel β-sheet flanked by several helices. The second subunit is illustrated in a molecular surface representation to visualize the oligomeric contacts of the C-terminal segment (black). The cofactors FAD and ThDP with Mg^{2+} have a shortest distance of 7.2 Å and are drawn in yellow.

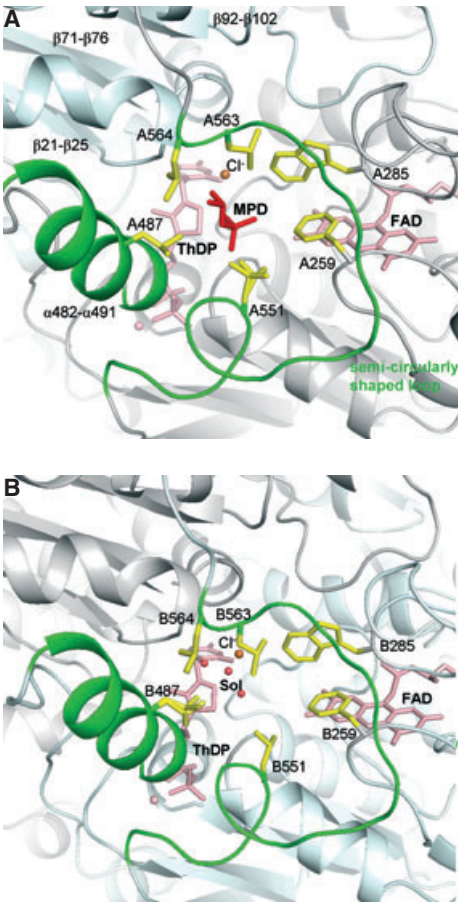

Fig. 3. Active site funnel. (A) In the open state containing the inhibitor MPD. The active site funnel is composed of two subunits (grey and blue-white); its entrance is formed by a semicircular loop segment of the C-terminal arm and helix B482:B491 both shown in green. The hydrophobic side chains constituting the pore are drawn in yellow. Other ThDP dependent enzymes have the active site pocket at the monomer–monomer interface. (B) In the closed state, without MPD bound. The closure is achieved by a conformational change of side chains LeuB487, LeuB551 and LeuB563.

might destabilize, in parallel, the simultaneous presence of an amino form at N4′ and a protonated C2 atom [31]. An invariant hydrogen bond between the GlyA424 carbonyl oxygen and the 4′-amino/imino group (2.8 Å in CDH) may assist by fine-tuning the position of the imino group (Fig. 4). The conserved residue GluB52 stabilizes the 4′-imino tautomeric form of the pyrimidine ring [7,8] by a strong hydrogen bond between the OE1 and N1′ atoms (their distance is 2.7 Å in CDH). Interestingly, in CDH (and in benzaldehyde lyase) the hydroxyl group of TyrA456 of the partner monomer is hydrogen bonded to the OE2 atom of GluB52, thereby adjusting its position and its pK_a value (Fig. 4). The OE1 atom is further linked to the polypeptide by invariant interactions.

The ThDP conformation and protein–ThDP interactions can be described very accurately due to the excellent resolution of the CDH structure. Although refinement was performed without any restraints between the ThDP atoms regarding their bond lengths and bond angles, the two ThDPs in the asymmetric unit are nearly identical (Fig. S2). The asymmetry of the two active sites suggested by the selective MPD binding (see below) is not reflected in the ThDP geometry at a resolution of 1.26 Å. Likewise, no

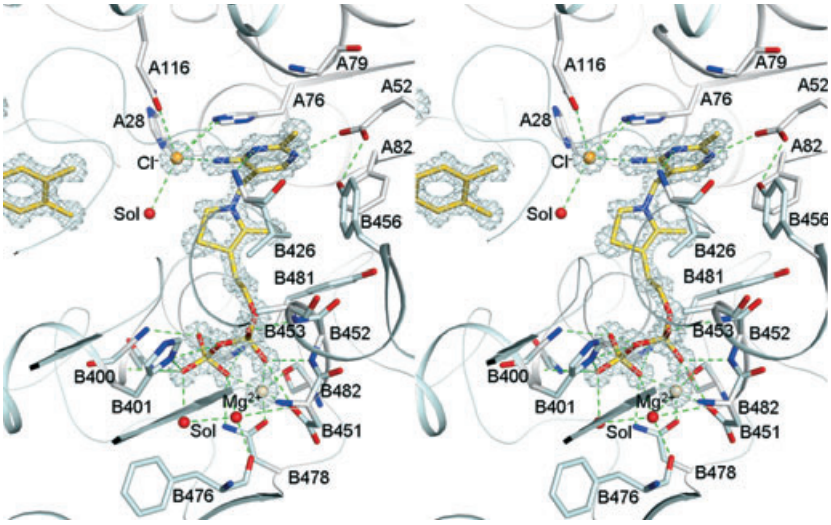

Fig. 4. Interaction between ThDP and the protein matrix. Hydrogen bonds are marked with green dashed lines indicating that the cofactor is mainly fixed by its diphosphate part. The electron density at 1.26 Å resolution is shown for ThDP, FAD, Mg^{2+} and Cl^{-} (contour level 1σ): FAD and ThDP in gold, the C, O and N atoms in light cyan (grey), red and blue, respectively; Cl^{-} in orange and Mg^{2+} in wheat. The residues contacting ThDP are well conserved throughout the enzyme family.

significant bond length differences are found between enzyme-bound ThDPs and between the enzyme-bound ThDP and free ThDP derived from high-resolution X-ray structures (Fig. S2).

The FAD cofactor is bound in an extended conformation at the C-terminal end of the six-stranded β-sheet of the domain β as reported for pyruvate oxidase [4] and acetohydroxy acid synthase [30]. FAD binding in CDH shows the characteristic features of the pyruvate oxidase structure family [22] where the conserved motif GxGxxG for dinucleotide binding is absent and the adenosine moiety of FAD binds to the second βαβαβ unit in the opposite direction. Nevertheless, the FAD binding mode varies substantially among the family members (in contrast to the strictly conserved ThDP binding) suggesting that its presence but not its exact binding characteristics is required. First, the structure of the irregular segment following strand A274:A279 in subunit β is substantially rearranged which considerably influences the location and orientation of the isoalloxazine ring. Second, the isoalloxazine ring of FAD is planar in CDH and acetohydroxy acid synthase but bent by 15° across the N^5–N^{10} axis in pyruvate oxidase. Third, solely in CDH FAD is largely shielded by the polypeptide scaffold. The access to the catalytic N5 atom is blocked by SerA240, PheA259, CysA260, TrpA285, PheA406 and LeuA551.

Substrate binding site

Kinetic studies under experimental conditions of crystal growth (40% (v/v) MPD, 15 mM Na^+ acetate, 200 mM NaCl, 1 mM ThDP, 1 mM NAD^+, 5 mM $MgCl_2$ and 100 μM CDO in 5 mM HEPES buffer, pH 7.0) revealed no specific activity for CDH raising the question which of the three main components of the crystallization buffer – NaCl, MPD or Na^+ acetate – is inhibiting catalysis.

The strongest inhibitory effect was observed for MPD (Fig. 5A), with 5% MPD leading to a decrease of the specific activity close to 60%; in the presence of 20% MPD, just 5% activity remained. This finding is reflected in the CDH structure where an MPD molecule is embedded into the potential substrate binding site of the open funnel (Fig. 3A). MPD is oriented in such a manner that its apolar part is directed towards the hydrophobic entrance. It contacts besides GlyA399 the apolar side chains of PheA259, TrpA285, LeuA551, LeuA487 and LeuA563. The first hydroxyl group of MPD is hydrogen bonded to HisB28 and the second interacts with the catalytic active C2 atom of ThDP, both at distances of 3.1 Å. Soaking experiments with substrate (3.7 mM CDO, 17 h) or co-crystallization experiments with up to 2 mM CDO did not lead to a displacement of the MPD molecule by the substrate. The strong binding of MPD to the active site is not too astonishing, since (a) MPD preferentially binds to hydrophobic sites [33], and (b) MPD resembles the monohydrated form of CDO not only in size but also with regard to the arrangement of the functional diol/dione substituents.

Interestingly, MPD is not present inside the closed substrate funnel that contains instead of the inhibitor three water molecules (Fig. 3B). This structural asymmetry in the two opposing active sites might be explained by a negative cooperativity with respect to the binding of MPD that would be in line with the concept of two communicating active sites in some ThDP enzymes [11]. A coupling between the active sites is also supported by the catalytic inactivity of

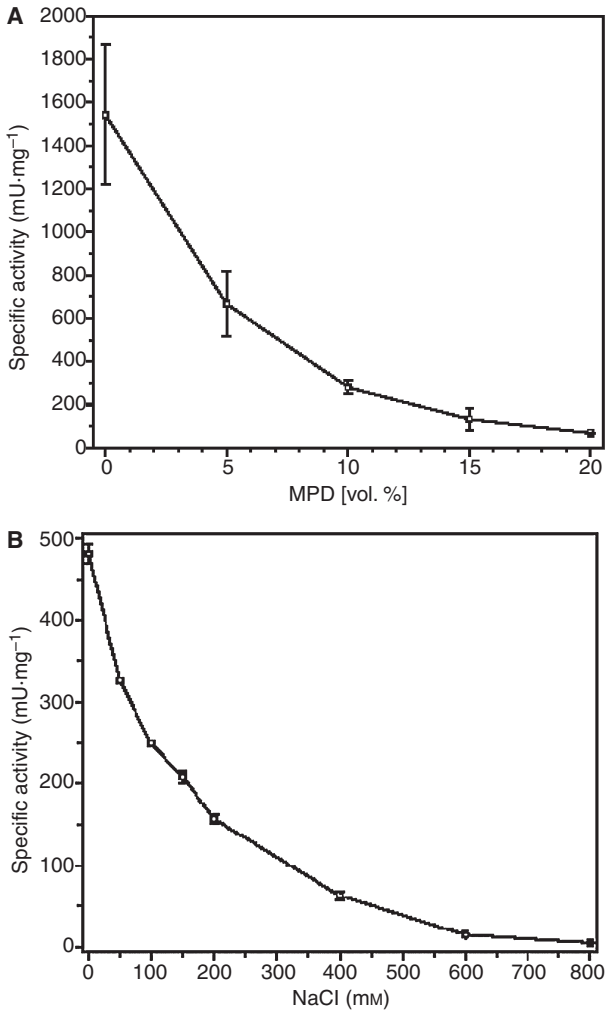

Fig. 5. Binding of inhibitors MPD and chloride. Influence of various concentrations of MPD (A) and NaCl (B) on the CDH specific activity: 0.7 μM CDH in 100 mM HEPES buffer, pH 8.0, plus 100 μM freshly thawed CDO, 1 mM NAD^+ and 0–20% MPD or 0–1 M NaCl, respectively. The incubation time was 5 min; 1 mU = nmol CDO·min^{-1}.

CDH in an MPD containing solution although one active site funnel is not occupied by MPD (albeit blocked for the substrate CDO in the crystalline state). Binding of substrate analogues exclusively into one active site were also found for yeast pyruvate decarboxylase [34] and the E1 component of *Thermus thermophilus* pyruvate dehydrogenase [35]. A mechanism of communication between the two active sites is not obvious in CDH because the ~ 20 Å long route between the aminopyrimidine rings does not appear to be optimized for an efficient proton transfer that is necessary for running two alternating catalytic cycles coupled by long-range acid/base catalysis [10,11]. In CDH this route is only lined up with a few protonable residues and not continuously water-filled as reported for the E1 component of pyruvate dehydrogenase [36] but rather blocked by Leu53, Leu82, Ala85, Ile425 and Tyr456 of both subunits.

Enzymatic activity studies with CDH indicated a significant but weaker inhibition by NaCl compared with MPD (Fig. 5). With 400 mM NaCl the specific activity was reduced to 10% which can be correlated with the structural finding of a putative chloride ion 3.3 Å apart from the C2 atom of ThDP in both substrate funnels (Figs 3 and 4). This assignment is consistent with the composition of the crystallization solution, the height and the spherical shape of the $2F_o - F_c$ electron density, the bond distances between 3.15 and 3.3 Å to neighbouring atoms, and the positively charged character of the protein environment. Polar interactions are formed between the chloride anion and the C2 and N4′ atoms of ThDP, the side chains of HisB76 and GlnB116 and a water molecule (Fig. 4). Notably, the chloride ion also interacts with the hydroxyl groups of MPD (distances 3.4 Å and 3.6 Å) in the open funnel that presumably enhances the affinity of both MPD and chloride in a synergistic fashion (Fig. 3A). The positions of the chloride ion and MPD might be normally occupied by the substrate CDO whose binding mode has, so far, not been structurally characterized. It is very likely, however, that HisB28, HisB31, HisB76, GlnB116 and AsnA484 are crucial for substrate binding and activation.

In contrast, Na^+ acetate substantially influences the enzyme activity only at concentrations higher than 15 mM and is not responsible for the inactivity of the enzyme in the crystallization solution (data not shown). However, at higher concentrations, it might occupy the assumed binding site for the chloride anion. Additionally, we found one MPD molecule, one chloride anion and one acetate at the dimer–dimer interface near crystal packing contacts emphasizing their importance for crystal formation.

Towards the reaction mechanism of CDH

CDH catalyses two reactions: the hydrolytic cleavage of the CDO ring to 6-oxohexanoate and the NAD^+ dependent oxidation of the semialdehyde 6-oxohexanoate to adipate (Fig. 1). Although the binding of CDO could not be experimentally established we assume that the orientation of CDO is largely determined since its hydrophobic portion probably points to the hydrophobic funnel entrance and its polar carbonyl groups to the hydrophilic base as found for MPD. The chloride ion might occupy the position of the C1 atom of CDO which is negatively charged in an intermediate state of

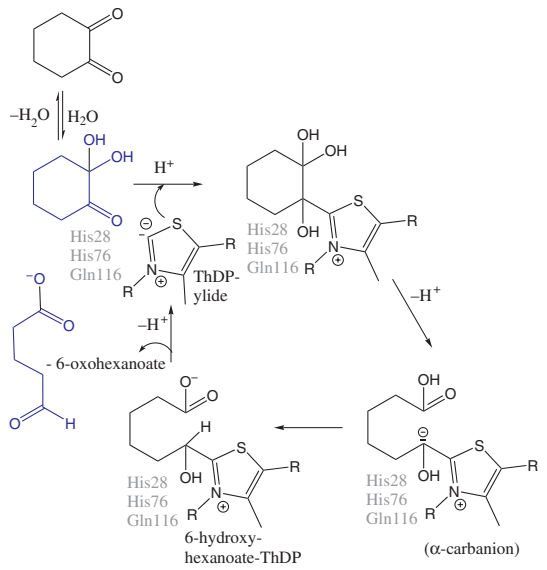

Fig. 6. Proposed mechanism of the CDH reaction. The ring cleavage is started by a nucleophilic attack of the C2 anion of activated ThDP onto the carbonyl group of CDO. Subsequently, the C–C bond of the aliphatic ring is cleaved thereby generating an α-carbanion. In the following step, the α-carbanion intermediate is protonated yielding 6-hydroxy-hexanoate-ThDP which is released to the product 6-oxohexanoate. The substrate CDO exists in solution in two forms, the unhydrated monoenol and the monohydrated ketone [52,53]. First kinetic studies indicate that the monohydrated ketone is the preferred substrate of CDH [18].

the established catalytic cycle of ThDP dependent enzymes [6]. In line with the mechanism reported for other family members [1,2] we postulated a nucleophilic attack of the C2 anion of activated ThDP onto the carbonyl group of CDO, a subsequent cleavage of the aliphatic ring and the release of the product 6-oxohexanoate accompanied by proton transfer steps (Fig. 6). HisB28, HisB76 and GlnB116 are attractive candidates to increase the electrophilic character of the attacked carbonyl carbon of CDO and to supply/uptake a proton towards/from the substrate–ThDP adduct during 6-oxohexanoate formation (Fig. 4).

The NAD^+ dependent reaction does not appear to proceed as expected since several experimental observations strongly suggest that the FAD cofactor does not participate in the redox process. First, with known reductants including ascorbate, NADH, Na^+ dithionite, Ti(III) citrate or $NaBH_4$, FAD cannot, or can only partially, be reduced [18]. Second, the N5 atom of the isoalloxazine ring is completely shielded by residues PheA259 and CysA260 and therefore inaccessible for both NAD^+ and 6-oxohexanoate, the latter being about 5 Å away from FAD. Third, in the structurally related ThDP dependent flavoenzymes glyoxylate carboligase and acetohydroxy acid synthase [15,16] (but not in pyruvate oxidase) the flavin cofactor is considered as an evolutionary relict that is important for structural reasons but does not participate in a redox reaction. This is not too uncommon and has been reported for other flavoenzymes [37]. However, solely in CDH, the paradox situation exists that a redox reaction is performed by the enzyme carrying FAD at the active site but without its participation. Although the current data clearly point to a direct hydride transfer between 6-oxohexanoate and NAD^+ and not to stepwise electron transfer via FAD (as proved for pyruvate oxidase and acetohydroxy acid synthase [38]), there is no space for NAD^+ in the active site funnel. Thus, either larger conformational changes to let NAD^+ in or a movement of 6-oxohexanoate out of the funnel must occur. Undoubtedly, the elucidation of the mechanism of the NAD^+ dependent reaction requires further studies, in particular the determination of the structure of the CDH–6-oxohexanoate–NAD^+ ternary complex.

Material and methods

Purification, enzymatic assay and crystallization

CDH was purified from *Azoarcus* sp. strain 22Lin [18] and stored in 50 mM MES buffer, pH 6.5, containing 1 mM $MgCl_2$ and 0.5 mM ThDP. Enzymatic activity was determined by monitoring the reduction of NAD^+ at 365 nm. Assays contained 100 mM HEPES buffer, pH 8.0, 1 mM NAD^+ and 0.1 mM CDO. After incubation for 5 min at 37 °C, reactions were started by addition of CDH [18]. Crystals grew at 25 °C by the hanging-drop method. The drop consisted of equal volumes of protein storage and reservoir solution, the latter composed of 60% MPD, 20 mM Na^+ acetate and 200 mM NaCl. The tetragonal crystals belong to the space group $P4_12_12$ with axes lengths a = 123.6 Å and c = 144.6 Å. A second cubic crystal form was obtained at 20 °C with a reservoir solution containing 17–18% (w/v) poly(ethylene glycol) (PEG 8000), 100 mM Na^+ acetate, 10 mM $MnCl_2$ and 2% (w/v) isopropanol in 0.1 M HEPES buffer, pH 7.5.

Data collection and phase determination

Native and MAD/SAD data were collected at the ID29 and ID14-4 beamlines at the European Synchrotron Radiation Facility (ESRF) (Grenoble) and MIR data inhouse using a Rigaku 200 rotating anode generator (see Table 1). Data processing was performed with the HKL and XDS packages [39,40]. Initially, two mercury positions were determined from the peak data set measured from CDH

crystals soaked with Hg(II) acetate (SHELXD [41]). Three platinum sites from CDH crystals soaked with K_2PtCl_4 were obtained from anomalous difference Fourier calculations. Due to the low occupancy of both heavy atom compounds two additional derivate data sets with 'pip' and 'terpy' soaked crystals were necessary for successful phasing (Table 1) using SHARP [42]. The figure of merit was 0.57 (0.58) for the centric (acentric) reflections over the resolution range 20–4 Å. Phases were improved by the solvent flattening procedure of SOLOMON [43] implemented into SHARP. On the basis of the resulting electron density map, the position of the heavy atoms and an approximate superposition with *L. plantarum* pyruvate oxidase one monomer could be masked and the non-crystallographic symmetry operator determined. After two-fold molecular averaging using DM [44] 30% of the polypeptide chain could be automatically incorporated into the electron density map with MAID [45]. The missing residues were built within O [46]. Data of the cubic crystal form were phased by the molecular replacement method [47].

Refinement and quality of the structure

The resulting model was initially refined with CNS-1.1 [48], using established molecular dynamics and least-squares minimization protocols. Non-crystallographic symmetry restraints were not applied. Water molecules and alternative amino acid conformations were incorporated and anisotropic temperature factor values were calculated with SHELXL-97 [49] (Table 1). The final model consists of 2 × 587 amino acid residues, two FAD molecules, two ThDP molecules, two Mg ions and 1185 water molecules. Additionally, three chloride ions, three MPD molecules and one acetate molecule from the crystallization buffer were detected in the crystal structure of CDH. A second conformation was obtained for 68 amino acid residues. According to PROCHECK [50] no dihedral angle of non-glycine and non-proline residues was located in disallowed regions. The structure of the cubic crystal form was refined using REFMAC5 [51].

Acknowledgements

This work was supported by the Max-Planck-Gesellschaft (JH, UE) and by the Deutsche Forschungsgesellschaft (PK, UE). We thank Christina Probian for the cultivation of *Azoarcus*, the staff of the beamlines ID29 and ID14-4 at ESRF (Grenoble) for help during data collection and Hartmut Michel for continuous support.

References

1 Jordan F (2003) Current mechanistic understanding of thiamin diphosphate-dependent enzymatic reactions. *Nat Prod Rep* **20**, 184–201.
2 Kluger R & Tittmann K (2009) Thiamin diphosphate catalysis: enzymic and nonenyzmic covalent intermediates. *Chem Rev* **108**, 1797–1833.
3 Lindqvist Y, Schneider G, Ermler U & Sundstrom M (1992) Three-dimensional structure of transketolase, a thiamine diphosphate dependent enzyme, at 2.5 Å resolution. *EMBO J* **11**, 2373–2379.
4 Muller YA & Schulz GE (1993) Structure of the thiamine- and flavin-dependent enzyme pyruvate oxidase. *Science* **259**, 965–967.
5 Dyda F, Furey W, Swaminathan S, Sax M, Farrenkopf B & Jordan F (1993) Catalytic centers in the thiamin diphosphate dependent enzyme pyruvate decarboxylase at 2.4 Å resolution. *Biochemistry* **32**, 6165–6170.
6 Nemeria NS, Chakraborty S, Balakrishnan A & Jordan F (2009) Reaction mechanisms of thiamin diphosphate enzymes: defining states of ionization and tautomerization of the cofactor at individual steps. *FEBS J* **276**, 2432–2446.
7 Wikner C, Meshalkina L, Nilsson U, Nikkola M, Lindqvist Y, Sundstrom M & Schneider G (1994) Analysis of an invariant cofactor-protein interaction in thiamin diphosphate-dependent enzymes by site-directed mutagenesis. Glutamic acid 418 in transketolase is essential for catalysis. *J Biol Chem* **269**, 32144–32150.
8 Kern D, Kern G, Neef H, Tittmann K, Killenberg-Jabs M, Wikner C, Schneider G & Hubner G (1997) How thiamine diphosphate is activated in enzymes. *Science* **275**, 67–70.
9 Kaplun A, Binshtein E, Vyazmensky M, Steinmetz A, Barak Z, Chipman DM, Tittmann K & Shaanan B (2008) Glyoxylate carboligase lacks the canonical active site glutamate of thiamine-dependent enzymes. *Nat Chem Biol* **4**, 113–118.
10 Jordan F, Nemeria NS & Sergienko E (2005) Multiple modes of active center communication in thiamin diphosphate-dependent enzymes. *Acc Chem Res* **38**, 755–763.
11 Frank RA, Leeper FJ & Luisi BF (2007) Structure, mechanism and catalytic duality of thiamine-dependent enzymes. *Cell Mol Life Sci* **64**, 892–905.
12 Widmann M, Radloff R & Pleiss J (2010) The thiamine diphosphate dependent Enzyme Engineering Database: a tool for the systematic analysis of sequence and structure relations. *BMC Biochem* **11**, 9.
13 Muller M, Gocke D & Pohl M (2009) Thiamin diphosphate in biological chemistry: exploitation of diverse thiamin diphosphate-dependent enzymes for asymmetric chemoenzymatic synthesis. *FEBS J* **276**, 2894–2904.
14 Tittmann K (2009) Reaction mechanisms of thiamin diphosphate enzymes: redox reactions. *FEBS J* **276**, 2454–2468.
15 Duggleby RG & Pang SS (2000) Acetohydroyacid synthase. *J Biochem Mol Biol* **33**, 1–36.

16 Chung ST, Tan RT & Suzuki I (1971) Glyoxylate carboligase of *Pseudomonas oxalaticus*. A possible structural role for flavine-adenine dinucleotide. *Biochemistry* **10**, 1205–1209.
17 Harder J & Probian C (1997) Anaerobic mineralization of cholesterol by a novel type of denitrifying bacterium. *Arch Microbiol* **167**, 269–274.
18 Steinbach AK, Fraas S, Harder J, Tabbert A, Brinkmann H, Meyer A, Ermler U & Kroneck PM (2011) Cyclohexane-1,2-dione hydrolase from denitrifying *Azoarcus* sp. strain 22Lin, a novel member of the thiamine diphosphate enzyme family. *J Bacteriol* **193**, 6760–6769.
19 Yoshida K, Yamaguchi M, Morinaga T, Kinehara M, Ikeuchi M, Ashida H & Fujita Y (2008) myo-Inositol catabolism in *Bacillus subtilis*. *J Biol Chem* **283**, 10415–10424.
20 Yoshida KI, Aoyama D, Ishio I, Shibayama T & Fujita Y (1997) Organization and transcription of the myo-inositol operon, iol, of Bacillus subtilis. *J Bacteriol* **179**, 4591–4598.
21 Hawkins CF, Borges A & Perham RN (1989) A common structural motif in thiamin pyrophosphate-binding enzymes. *FEBS Lett* **255**, 77–82.
22 Dym O & Eisenberg D (2001) Sequence-structure analysis of FAD-containing proteins. *Protein Sci* **10**, 1712–1728.
23 Yagari Y (1961) Metabolism of cyclohexane-diol-*trans*-1,2 by soil bacterium. *Biken J* **4**, 197–207.
24 Dangel W, Tschech A & Fuchs G (1988) Anaerobic metabolism of cyclohexanol by denitrifying bacteria. *Arch Microbiol* **150**, 358–362.
25 Muller YA, Lindqvist Y, Furey W, Schulz GE, Jordan F & Schneider G (1993) A thiamin diphosphate binding fold revealed by comparison of the crystal structures of transketolase, pyruvate oxidase and pyruvate decarboxylase. *Structure* **1**, 95–103.
26 Holm L & Sander C (1993) Protein structure comparison by alignment of distance matrices. *J Mol Biol* **233**, 123–138.
27 McCourt JA, Pang SS, King-Scott J, Guddat LW & Duggleby RG (2006) Herbicide-binding sites revealed in the structure of plant acetohydroxyacid synthase. *Proc Natl Acad Sci USA* **103**, 569–573.
28 Mosbacher TG, Mueller M & Schulz GE (2005) Structure and mechanism of the ThDP-dependent benzaldehyde lyase from *Pseudomonas fluorescens*. *FEBS J* **272**, 6067–6076.
29 Neumann P, Weidner A, Pech A, Stubbs MT & Tittmann K (2008) Structural basis for membrane binding and catalytic activation of the peripheral membrane enzyme pyruvate oxidase from *Escherichia coli*. *Proc Natl Acad Sci USA* **105**, 17390–17395.
30 Pang SS, Guddat LW & Duggleby RG (2003) Molecular basis of sulfonylurea herbicide inhibition of acetohydroxyacid synthase. *J Biol Chem* **278**, 7639–7644.
31 Berthold CL, Moussatche P, Richards NG & Lindqvist Y (2005) Structural basis for activation of the thiamin diphosphate-dependent enzyme oxalyl-CoA decarboxylase by adenosine diphosphate. *J Biol Chem* **280**, 41645–41654.
32 Hasson MS, Muscate A, McLeish MJ, Polovnikova LS, Gerlt JA, Kenyon GL, Petsko GA & Ringe D (1998) The crystal structure of benzoylformate decarboxylase at 1.6 Å resolution: diversity of catalytic residues in thiamin diphosphate-dependent enzymes. *Biochemistry* **37**, 9918–9930.
33 Anand K, Pal D & Hilgenfeld R (2002) An overview on 2-methyl-2,4-pentanediol in crystallization and in crystals of biological macromolecules. *Acta Crystallogr D Biol Crystallogr* **58**, 1722–1728.
34 Lu G, Dobritzsch D, Baumann S, Schneider G & Konig S (2000) The structural basis of substrate activation in yeast pyruvate decarboxylase. A crystallographic and kinetic study. *Eur J Biochem* **267**, 861–868.
35 Nakai T, Nakagawa N, Maoka N, Masui R, Kuramitsu S & Kamiya N (2004) Ligand-induced conformational changes and a reaction intermediate in branched-chain 2-oxo acid dehydrogenase (E1) from *Thermus thermophilus* HB8, as revealed by X-ray crystallography. *J Mol Biol* **337**, 1011–1033.
36 Frank RA, Titman CM, Pratap JV, Luisi BF & Perham RN (2004) A molecular switch and proton wire synchronize the active sites in thiamine enzymes. *Science* **306**, 872–876.
37 Bornemann S (2002) Flavoenzymes that catalyse reactions with no net redox change. *Nat Prod Rep* **19**, 761–772.
38 Tittmann K, Schroder K, Golbik R, McCourt J, Kaplun A, Duggleby RG, Barak Z, Chipman DM & Hubner G (2004) Electron transfer in acetohydroxy acid synthase as a side reaction of catalysis. Implications for the reactivity and partitioning of the carbanion/enamine form of (alpha-hydroxyethyl)thiamin diphosphate in a 'nonredox' flavoenzyme. *Biochemistry* **43**, 8652–8661.
39 Otwinowski Z & Minor W (1997) Processing of X-ray diffraction data collected in oscillation mode. *Macromol Crystallog* **276**, 307–326.
40 Kabsch W (1993) Automatic processing of rotation diffraction data from crystals of initially unknown symmetry and cell constants. *J Appl Cryst* **26**, 795–800.
41 Schneider TR & Sheldrick GM (2002) Substructure solution with SHELXD. *Acta Crystallogr D Biol Crystallogr* **58**, 1772–1779.
42 De la Fortelle E & Bricogne G (1997) Maximum likelihood heavy-atom parameter refinement for multiple isomorphous replacement and multiwavelength

anomalous diffraction methods. *Methods Enzymol* **276**, 472–494.
43 Abrahams JP & Leslie AG (1996) Methods used in the structure determination of bovine mitochondrial F1 ATPase. *Acta Crystallogr D Biol Crystallogr* **52**, 30–42.
44 Cowtan KD (1994) 'DM': an automated procedure for phase improvement by density modification. *Joint CCP4 and ESF-EACBM Newsletter on Protein Crystallography*, **3**, 34–38.
45 Levitt DG (2001) A new software routine that automates the fitting of protein X-ray crystallographic electron-density maps. *Acta Crystallogr D Biol Crystallogr* **57**, 1013–1019.
46 Jones TA, Zou JY, Cowan SW & Kjeldgaard M (1991) Improved methods for building protein models in electron density maps and the location of errors in these models. *Acta Crystallogr A* **47**, 110–119.
47 Kissinger CR, Gehlhaar DK & Fogel DB (1999) Rapid automated molecular replacement by evolutionary search. *Acta Crystallogr D Biol Crystallogr* **55**, 484–491.
48 Brunger AT, Adams PD, Clore GM, DeLano WL, Gros P, Grosse-Kunstleve RW, Jiang JS, Kuszewski J, Nilges M, Pannu NS *et al.* (1998) Crystallography and NMR system: a new software suite for macromolecular structure determination. *Acta Crystallogr D Biol Crystallogr* **54**, 905–921.
49 Sheldrick GM & Schneider TR (1997) SHELXL: high-resolution refinement. *Methods Enzymol* **277**, 319–343.
50 Laskowski RA, MacArthur MW, Moss DS & Thornton JM (1993) PROCHECK: a program to check the stereochemical quality of protein structures. *J Appl Cryst* **26**, 283–291.
51 Murshudov GN, Vagin AA & Dodson EJ (1997) Refinement of macromolecular structures by the maximum-likelihood method. *Acta Crystallogr D Biol Crystallogr* **53**, 240–255.
52 Bakule R & Long FA (1963) Keto-enol transformation of 1,2-cyclohexanedione. I. Hydration and keto-enol equilibria. *J Am Chem Soc* **85**, 2309–2312.
53 Long FA & Bakule R (1963) Keto-enol transformation of 1,2-cyclohexanedione. II. Acid catalysis in strongly acidic media. *J Am Chem Soc* **85**, 2313–2318.

Supporting information

The following supplementary material is available:
Fig. S1. Molecular surface representation of CDH.
Fig. S2. Conformation of the ThDP cofactor.

This supplementary material can be found in the online version of this article.

Please note: As a service to our authors and readers, this journal provides supporting information supplied by the authors. Such materials are peer-reviewed and may be reorganized for online delivery, but are not copy-edited or typeset. Technical support issues arising from supporting information (other than missing files) should be addressed to the authors.